Neurobiology of Aging 95 (2020) 168–175

Contents lists available at ScienceDirect

Neurobiology of Aging

journal homepage: www.elsevier.com/locate/neuaging

Changes in the intracellular microenvironment in the aging human brain

Dinesh K. Deelchand[a,*], J. Riley McCarten[b,c], Laura S. Hemmy[b,d], Edward J. Auerbach[a], Lynn E. Eberly[e], Małgorzata Marjańska[a]

[a] Center for Magnetic Resonance Research, Department of Radiology, University of Minnesota, Minneapolis, MN, USA
[b] Geriatric Research, Education and Clinical Center, Veterans Affairs Health Care System, Minneapolis, MN, USA
[c] Department of Neurology, University of Minnesota, Minneapolis, MN, USA
[d] Department of Psychiatry, University of Minnesota, Minneapolis, MN, USA
[e] Division of Biostatistics, University of Minnesota, Minneapolis, MN, USA

ARTICLE INFO

Article history:
Received 9 April 2020
Received in revised form 23 June 2020
Accepted 19 July 2020
Available online 25 July 2020

Keywords:
ADC
Diffusion
T_2
Magnetic resonance spectroscopy
Young

ABSTRACT

Normal brain aging is associated with changes occurring at all levels. This study investigates age-related differences in the brain intracellular microenvironment by comparing the apparent diffusion coefficients (ADC) and apparent transverse relaxation time constants (T_2) of 5 neurochemicals (i.e., total *N*-acetyl-aspartate, total creatine, total choline, glutamate, and *myo*-inositol) between young and older adults. Thirty-two young healthy adults (18–22 years) and 26 older healthy adults (70–83 years) were recruited. Three brain regions were studied at 3 T: prefrontal, posterior cingulate and occipital cortices. ADC and T_2 were measured using stimulated echo acquisition mode and localization by adiabatic selective refocusing sequences, respectively. This study shows that the diffusivities of several neurochemicals are higher in older than in younger adults. In contrast, shorter apparent T_2 values for several metabolites were measured in older adults. Age-related difference in ADC and apparent T_2 of metabolites seem to be region-specific. Furthermore, this study shows that it is feasible to observe age-related differences in the cellular microenvironment of neurochemicals in the normal aging brain.

1. Introduction

Normal brain aging is associated with changes occurring at all levels from molecular to morphological, for example, changes in blood flow and metabolism, decline in a number of cognitive functions, changes in the volume of the brain, the amount of white matter (WM), and an increase in the cerebral iron content (Peters, 2006). All of these changes occur to a different extent in the entire human brain.

Magnetic resonance imaging (MRI) is a non-invasive imaging modality, which has been widely used for volumetric and morphometric analysis of the brain. Using structural MRI, it was previously demonstrated that brain volume changes correlate with age (Walhovd et al., 2011). Interestingly, the prefrontal cortex (PFC) was found to be the most affected region while occipital cortex (OCC) and posterior cingulate cortex (PCC) were the least affected regions (Fjell and Walhovd, 2010), consistent with the cognitive changes observed in the normal aging brain. In addition, diffusion-weighted imaging (DWI) assessing brain tissue microstructure showed that the apparent diffusion coefficients (ADC) of water gradually increased from young adulthood into late life (Klimas et al., 2013; Watanabe et al., 2013). On the other hand, fractional anisotropy, which is a measure of structural macroscopic anisotropy in the brain, was found to decrease with age in the frontal, parietal, and temporal lobes (Grieve et al., 2007).

Proton magnetic resonance spectroscopy (^{1}H MRS) is a technique which allows for non-invasive measurement of age-associated neurochemical concentrations in vivo in the brain (Marjańska et al., 2017). The most commonly measured neurochemicals are *N*-acetyl-aspartate (NAA), total creatine (tCr, creatine plus phosphocreatine), total choline (tCho, phosphorylcholine plus glycerophosphorylcholine), glutamate (Glu), and *myo*-inositol (mIns). These neurochemicals are preferentially concentrated in certain cell types: for example, NAA and Glu are predominantly located in neurons, tCr and tCho are found in both neuronal and glial cells, while mIns is thought to be localized exclusively in astrocytes (de Graaf, 2007; Ligneul et al., 2019). Age-related differences in neurochemical concentrations are also region-specific (Marjańska et al., 2017) where NAA and Glu were lower with age in OCC while mIns and tCr were higher with age in PCC.

* Corresponding author at: Center for Magnetic Resonance Research, University of Minnesota, 2021 6th St SE, Minneapolis, MN 55455, USA. Tel.: +1 612 625 8097; fax: +1 612 626 2004.
E-mail address: deelc001@umn.edu (D.K. Deelchand).

0197-4580/$ – see front matter © 2020 Elsevier Inc. All rights reserved.
https://doi.org/10.1016/j.neurobiolaging.2020.07.017

The cellular microenvironment of neurochemicals can be examined using advanced MRS techniques such as diffusion-weighted (DW) -MRS and transverse (T_2) relaxometry. The ADC value as measured by DW-MRS reflects the molecular displacement motion within the intracellular space (Ronen and Valette, 2015). By probing the diffusivity of metabolites, specific information on compartmentalization can be obtained at both cellular and sub-cellular levels (Palombo et al., 2018b; Valette et al., 2018). On the other hand, T_2 relaxation is a result of nuclear spin-spin interactions as reflected by MRS signal decay with time. T_2 is very sensitive to changes in molecular motion primarily through interaction of metabolites with structural or systolic macromolecules (Öngür et al., 2010).

With DW-MRS, we recently reported that the diffusivity of 5 major metabolites (NAA, tCr, tCho, Glu, and mIns) can be measured at 3 T (Deelchand et al., 2018b). Previously, it was demonstrated that the ADC of tNAA, tCr, and tCho was lower in older adults (Zheng et al., 2012). However, no difference in the ADC of water was found between the young and older cohorts, which is contradictory to previous DWI studies (Klimas et al., 2013; Watanabe et al., 2013). Several studies have reported the apparent T_2 relaxation time constants of metabolites with contradicting results in the older adult brains (Christiansen et al., 1993; Kirov et al., 2008; Kreis et al., 2005). We previously showed that apparent T_2 of NAA, tCr, and tCho can be measured reliably at high field strength, and these T_2 values were shorter in older adults by 10%–23% in the OCC (Marjańska et al., 2013).

Therefore, the aims of this study are to compare trace/3 ADC values (i.e., averaged ADC along 3 orthogonal directions) and apparent T_2 relaxation time constants of the 5 major metabolites and water in the human brain between young and older adults in 3 brain regions: PCC, OCC, and PFC.

2. Methods

2.1. Subjects

Thirty-two young adults (9 males; age: 21 ± 1 years, range 18–22) and 26 older adults (11 males; age: 74 ± 3 years, range 70–83) were recruited after providing informed consent for the study approved by the Human Subjects Protection Committee at the University of Minnesota Institutional Review Board. All subjects completed a medical history questionnaire validated to recruit healthy older adults for cognitive research (Christensen et al., 1992) and controls for central nervous system and cardiovascular disease, and were screened for cognitive impairment with the Montreal Cognitive Assessment (Nasreddine et al., 2005). Study exclusions included Montreal Cognitive Assessment scores <24, neurological disorders (e.g., stroke, neurodegenerative conditions, epilepsy), a history of psychiatric diagnoses, or current psychotropic medication use. Older adults were further evaluated with a neuropsychological battery to rule out any previously undetected cognitive deficits: Trail Making Test (Reitan, 1979), Digit Span Forward (Wechsler, 1997), Stoop (Golden, 1978), Boston Naming Test (Kaplan et al., 1983), verbal fluency (Benton et al., 1994), California verbal learning test (Delis et al., 2000), Rey Complex Figure (Meyers and Meyers, 1995), Logical Memory (Wechsler, 1987), Block Design (Wechsler, 1997), Digit Symbol (Wechsler, 1997), Information (Wechsler, 1997), and American version of the Nelson adult reading test (Grober et al., 1991). Young adults were evaluated with an abbreviated version of the older adult battery to rule out any gross cognitive deficits (Information, Digit Span, Block Design, Digit Symbol, verbal fluency, California verbal learning test).

ADC and T_2 data were collected from 3 different brain regions in all subjects using the 2 MRS acquisition protocols in 2 randomized sessions. The order in which information from different brain regions was obtained was also randomized between subjects. Both sessions were carried out within 5 weeks. T_2 data were missing from 1 subject in each group since the 2 subjects did not come back for their measurements.

2.2. MR acquisition

All MR measurements were carried out on a whole-body 3 T Siemens Prisma$_{Fit}$ system (Siemens Medical Solutions, Erlangen, Germany). The standard body coil was used for radiofrequency excitation while the 32-channel receive-only head coil was used for signal reception.

ADC and T_2 data were acquired from 3 volumes-of-interest (VOIs): PCC (2.5 × 2.5 × 2.5 cm^3), OCC (3 × 2.3 × 2.3 cm^3), and PFC (2.5 × 2.5 × 2.5 cm^3) (Supplementary Fig. 1). For high reproducibility of voxel placement between acquisitions, the vendor-provided automatic voxel positioning technique called AutoAlign was utilized (van der Kouwe et al., 2005).

In each session, magnetization-prepared rapid gradient-echo images (1 mm^3 isotropic resolution; repetition time, T_R = 2530 ms; echo time, T_E = 3.65 ms; inversion time, T_I = 1100 ms; flip angle = 7°; GRAPPA acceleration factor = 2) were acquired to position the VOIs. First- and second-order shims were automatically adjusted for each VOI using the system 3D gradient-echo shim, operated in the "Brain" mode. In addition, the B_1 field for the 90° pulse and the water suppression flip angles were calibrated for each VOI.

ADC data were measured using stimulated echo acquisition mode (STEAM, $T_E/T_M/T_R$ = 21.22/105/3000 ms) as previously described (Deelchand et al., 2018b). Briefly, the water signal was suppressed using variable power radiofrequency pulses with optimized relaxation delays interleaved with outer volume suppression pulses. Diffusion weighting was applied using bipolar gradients in 3 orthogonal directions with positive gradients—that is, [1,1,–0.5], [1, –0.5,1], and [–0.5,1,1]—and negative gradients—that is, [–1,–1, 0.5], [–1,0.5,–1], and [0.5,–1,–1]—to remove cross-term effects. Single-shot metabolite spectra were acquired at 2 b-values: a null b-value (16 averages) and a high-nominal b-value (48 averages, 6 DW directions) of 3172 s/mm^2 in all 3 regions. The diffusion gradient duration was 5.85 ms operating at 70 mT/m with a diffusion time of 118 ms. Water reference scans at both b-values were also acquired for eddy current correction.

T_2 of metabolites and water were measured using localization by adiabatic selective refocusing (LASER, T_R = 3 seconds) as previously described (Deelchand et al., 2018a). Water suppression was also achieved with variable power radiofrequency pulses with optimized relaxation delays, but no outer volume suppression pulses were used in the pulse sequence. Metabolite spectra were acquired at 6 different T_Es: 35, 140, 230, 290, 330, and 400 ms with 8, 16, 32, 32, 64, and 128 averages, respectively. This non-uniform averaging scheme with more averages measured at longer T_E was used to have high signal-to-noise ratio (SNR) spectra at all TEs. Water reference scans were also acquired for eddy current correction and for the determination of the apparent T_2 of tissue water.

Individual single-shot spectra from both sessions were saved for further post-processing offline. All MRS data were acquired with 2048 complex data points using a spectral width of 6 kHz. The carrier frequency of the localization radiofrequency pulses was set to 3 ppm.

2.3. Tissue segmentation

Magnetization-prepared rapid gradient-echo images were segmented using the FMRIB Software Library (Jenkinson et al., 2012). Fractions of gray matter (GM), WM, and cerebrospinal fluid (CSF) in each VOI were determined using an in-house written algorithm in MATLAB (MathWorks Inc, Natick, MA). For example, the

GM fraction was estimated as the ratio of all voxels classified as GM to the total voxels in the VOI.

2.4. Spectral processing and quantification

All MR spectra were post-processed in MATLAB using the MRSpa package (https://www.cmrr.umn.edu/downloads/mrspa/). Eddy current effects were first corrected. For ADC data only, low SNR spectra were removed to avoid bias in the ADC values (Deelchand et al., 2018b). Single-shot frequency and phase corrections were then performed using cross-correlation and least-square algorithms. For the ADC data, spectra, at null *b*-value and for all 6 gradient diffusion directions, were summed separately. Similarly, spectra acquired at different T_Es were individually summed for the T_2 data.

All resulting spectra were analyzed with LCModel (Provencher, 1993) version 6.3-0G (Stephen Provencher Inc, Oakville, Canada) without applying any baseline correction, zero-filling, or apodization functions to the in vivo data. All spectra were fitted between 0.5 and 4.1 ppm.

Basis sets for STEAM and LASER at 6 different T_Es were simulated using custom software in MATLAB based on density matrix formalism (Henry et al., 2006) using measured and published chemical shift and *J*-coupling values (Govind et al., 2015).

The basis set for both sequences consisted of 19 metabolites: alanine, ascorbate, aspartate, creatine, γ-aminobutyric acid, glucose, Glu, glutamine, glutathione, glycerophosphorylcholine, mIns, *scyllo*-inositol, lactate, NAA, NAAG, phosphocreatine, phosphorylcholine, phosphorylethanolamine, and taurine. Separate basis spectra were generated for the singlet and multiplet (i.e., CH_3 and CH_2 groups) resonances of NAA: denoted as sNAA and mNAA, respectively. In addition, the CH_3 and CH_2 groups of creatine and phosphocreatine were separated for the T_2 analysis. Due to differences in the macromolecular pattern recently observed between young and older adults (Marjańska et al., 2018), the macromolecular spectra were measured from both cohorts using the metabolite-nulled technique in STEAM (2 young subjects with 704 averages, 2 older subjects with 1280 averages) and LASER (2 young subjects with 512 averages, 2 older subjects with 1536 averages). These macromolecular spectra were included in the basis sets for each sequence. A singlet peak was also simulated at 1.45 ppm within LCModel to account for the falx cerebri lipid signal (McIntyre et al., 2007) observed in several of the older adults. Metabolites with Cramer-Rao lower bounds <25% were selected for further analysis.

ADC values for tCr, tCho, tNAA, Glu, and mIns were calculated as the mean ADC in all 3 gradient diffusion directions after determining the ADC value in each gradient diffusion direction using the geometric mean of the metabolite signals measured with both gradient polarities as previously reported (Deelchand et al., 2018b). Water ADC was also determined from the integral of the eddy current corrected water peak.

The apparent T_2 values for tCr, tCho, tNAA, Glu, and mIns were obtained by fitting the LCModel amplitudes of these metabolites with an exponential decay function (Mlynarik et al., 2001). Since water T_2 values correspond to different environments, the T_2 of tissue water and T_2 of water in CSF in each subject were determined by fitting the integrals of the eddy current corrected water peak at each T_E with a bi-exponential function (Whittall et al., 1997) using the known CSF content in each VOI from segmentation.

2.5. Statistics

Apparent T_2, ADC, and tissue content data were summarized with means and standard deviations; no large outliers were seen. Young versus older groups were compared using a linear mixed model, fit for each T_2 and each ADC measure separately; each model included group, region, and their interaction, and allowed for group and region specific variances. Models were adjusted for sex. Diagnostics indicated that model assumptions were well met. Tissue (WM, GM) and CSF contents were compared within region between young and older groups using one-way analysis of variance. Bonferroni correction was used to control for multiple testings (6 neurochemicals in T_2 measurements and 5 neurochemicals in ADC measurements in the 3 brain regions), the threshold of significance was 0.0027 (0.05/18) and 0.0033 (0.05/15) for T_2 and ADC values of metabolites, respectively. The threshold of significance was 0.0083 (0.05/6) and 0.0167 for T_2 of water and ADC, respectively.

3. Results

3.1. ADC of metabolites and water

Typical DW STEAM spectra acquired from the PCC are shown in Fig. 1 for 1 young and 1 older adults. Excellent high-spectral quality, with minimal lipid contamination and flat baseline from efficient water suppression, was routinely obtained in this study. Consistent data quality was obtained in OCC and PCC as observed by the narrow water linewidths, with mean linewidths ranging from 6.0 to 8.5 Hz (Supplementary Table 1). However, the spectral linewidths were slightly broader in the PFC (mean linewidths ranging from 9.5 to 10.6 Hz) due to proximity of the frontal sinuses and nasal cavity, such that ADC data from 8 young and 14 older adults were excluded from further analysis.

At null *b*-value, similar spectral patterns with comparable SNR were observed between the young and older groups. At high *b*-value, even though the diffusion gradient strengths were identical in both cohorts, the spectral amplitudes were lower in older adults than young adults suggesting that ADC values of metabolites are higher in the older adult brain. The effects of cross-terms across the 3 diffusion directions are visible in the singlet peaks in the high *b*-value spectra (Fig. 1).

The measured ADC values for 5 major metabolites and water for young and older adults are reported in Table 1. No gender differences were observed between the cohorts. The ADC values for tNAA, tCr, tCho, and mIns were significantly higher ($p < 0.0033$) in older compared to young adults in the PCC, and the ADC was higher between 8% and 19%. Similarly, in the OCC, only tCr had significantly higher ADC values (8%, $p = 0.001$) in older adults. However, no significant difference in ADC values was observed for the 5 major metabolites in the PFC.

The ADC values of tissue water in all 3 brain regions were found to be 3.6%–6.8% higher in older adults with the largest difference observed in the PCC (Table 1).

3.2. T_2 of metabolites and water

LASER spectra acquired from 1 young and 1 older subject at different T_Es in the PCC are shown in Fig. 2. High-quality spectra were consistently measured within and between subjects similar to the ADC measurements. Comparable water linewidths as observed in the ADC measurements were found in the PCC and the OCC, while in the PFC, the water linewidth was slightly broader. Based on the water linewidth >10 Hz criterion, 9 young and 13 older T_2 datasets in the PFC region were excluded from further analysis.

Fig. 2 shows a noticeable difference in the peak heights of tNAA and tCr, especially visible at long echo times (>250 ms), suggesting that the apparent T_2s of these metabolites are different between 2 cohorts.

Contrary to higher ADC values observed for some metabolites in the older adults, the apparent T_2 relaxation times of metabolites were found to be shorter in older adults (Table 2). No gender

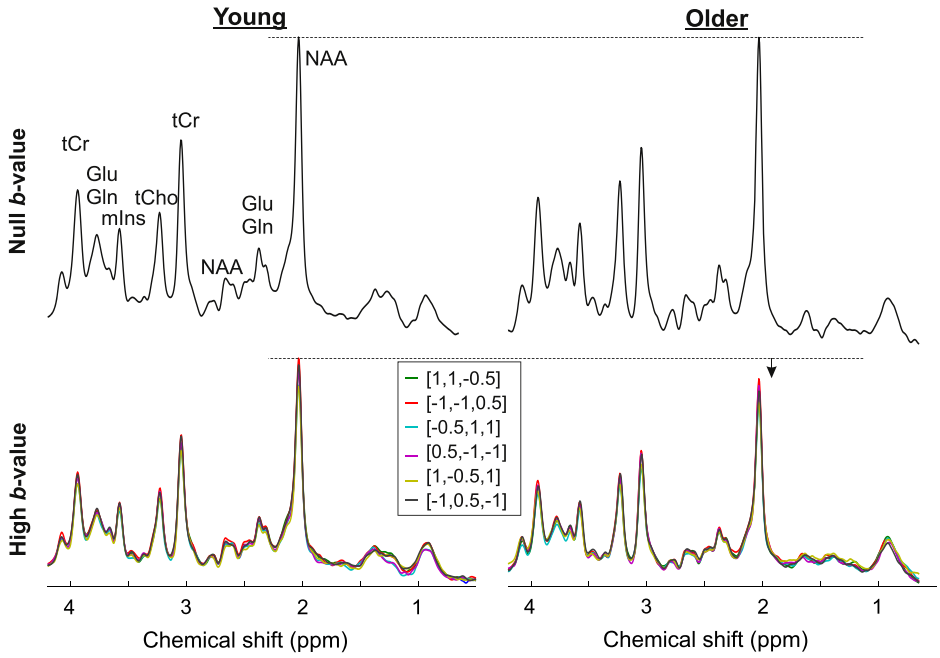

Fig. 1. Diffusion-weighted spectra from 1 young (20-year-old female) adult and 1 older (70-year-old female) adult acquired in the PCC using STEAM (T_R/T_E = 3000/21.2 ms) at 3 T. Spectra acquired at null *b*-value (16 averages, top) and at high *b*-value in all 6 directions (48 averages per direction, bottom) are shown. Note the excellent spectral quality, with no lipid contamination, flat baseline, and the high SNR at the high *b*-value. Abbreviations: PCC, posterior cingulate cortex; SNR, signal-to-noise ratio.

differences were observed between the cohorts. In the PCC, apparent T_2 of tNAA, tCr-CH_3, tCr-CH_2, tCho, and mIns were significantly lower ranging from 5% lower tCr-CH_3 to 11% lower NAA and tCr-CH_2. Similarly, in the OCC, significantly lower apparent T_2 values ($p < 0.0027$) were observed for tNAA, tCr-CH_3, tCr-CH_2, and mIns in the older adults' group, while Glu and tCho did not show any significant difference between the 2 groups.

The apparent T_2 of tissue water was significantly faster in the older cohort in all 3 regions studied (Table 2). On the other hand, the apparent T_2 of water in CSF was significantly faster in the young cohort in all 3 regions (Table 2).

3.3. Tissue content in VOIs

The VOI sizes for the regions studied were similar between the 2 age groups. Due to atrophy, the VOIs in the older adults contained a higher amount of CSF and a lower amount of GM (Fig. 3). Since a larger volume of the VOI was occupied by CSF, in which there are no metabolites except glucose and lactate, the contribution of metabolites coming from GM and WM was different between the groups. In older adults, metabolites coming from WM contributed more signal than in younger adults since WM content was higher by 14% in PCC, 8% in OCC, and 13% in PFC in older adults.

4. Discussion

The present study shows that region-specific differences occur in the intracellular microenvironment in older versus younger human brains. Mainly, the diffusivity of mIns, tCr, and tissue water was significantly higher in the older healthy adults than in young healthy adults. The apparent T_2 relaxation time constants of neurochemicals and tissue water were significantly shorter in the older cohort. These differences in ADC and T_2 metrics were region-specific, that is, PCC was the most sensitive region in both measurements, followed by OCC and then PFC.

The diffusivity of several neurochemicals and tissue water was faster in the healthy older versus younger brains. This is the first study reporting an increase in the ADC values for the major metabolites in older adults and is in disagreement with a previous study (Zheng et al., 2012) where a decrease in ADC of at least 25% was observed for NAA, tCr, and tCho. This discrepancy in metabolites' diffusivities might be related to several differences between the studies, such as the echo time, diffusion times, and VOI

Table 1
Trace/3 ADC values (mean ± SD) of metabolites and tissue water in the 2 age groups in 3 brain regions

Compound	Trace/3 ADC (μm^2/ms)								
	PCC			OCC			PFC		
	Young	Older	*p*-value	Young	Older	*p*-value	Young	Older	*p*-value
tNAA	0.12 ± 0.01	0.13 ± 0.02	**0.0014**	0.14 ± 0.01	0.14 ± 0.02	0.4573	0.13 ± 0.01	0.13 ± 0.03	0.5249
tCr	0.12 ± 0.01	0.14 ± 0.02	**0.0008**	0.13 ± 0.01	0.14 ± 0.01	**0.0010**	0.13 ± 0.01	0.13 ± 0.03	0.7324
tCho	0.11 ± 0.01	0.13 ± 0.03	**0.0019**	0.11 ± 0.02	0.13 ± 0.02	0.0242	0.11 ± 0.04	0.13 ± 0.05	0.1992
Glu	0.14 ± 0.02	0.15 ± 0.03	0.0133	0.15 ± 0.02	0.15 ± 0.02	0.7391	0.14 ± 0.02	0.13 ± 0.05	0.1423
mIns	0.12 ± 0.01	0.13 ± 0.02	**0.0011**	0.12 ± 0.01	0.13 ± 0.02	0.0329	0.12 ± 0.04	0.13 ± 0.05	0.2234
Tissue water	0.65 ± 0.02	0.69 ± 0.04	$\mathbf{4.5 \times 10^{-7}}$	0.62 ± 0.03	0.64 ± 0.03	**0.0039**	0.69 ± 0.03	0.72 ± 0.04	**0.0110**

Bold values denote statistical significance, i.e. $p < 0.0033$ for metabolites and $p < 0.0167$ for water.
Key: ADC, apparent diffusion coefficient; Glu, glutamate; mIns, myo-inositol; OCC, occipital cortex; PCC, posterior cingulate cortex; PFC, prefrontal cortex; SD, standard deviation; tCho, total choline; tCr, total creatine.

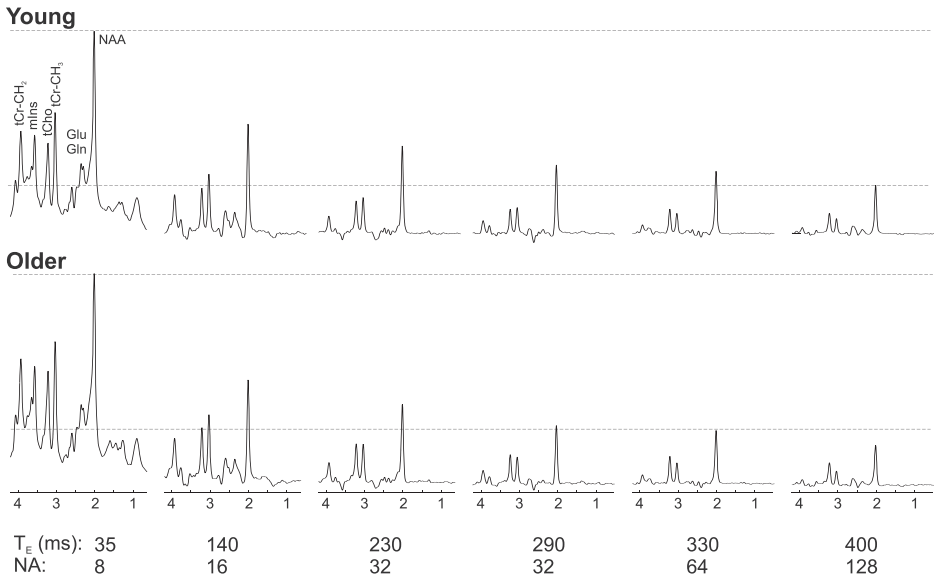

Fig. 2. LASER spectra ($T_R = 3$ s with different number of averages, NA) acquired at 6 T_Es from 1 young (22 F) adult and 1 older (73 F) adult in the PCC at 3 T. For display purposes, the spectra were normalized such that at the shortest T_E, the height of NAA peak was identical. The dashed lines show that the apparent T_2 of NAA and other singlets are shorter in older adult brain. Abbreviations: NAA, N-acetyl-aspartate; PCC, posterior cingulate cortex.

selection. The VOI used in the previous study contained mostly WM, while in the present study all VOIs contained a mixture of WM and GM. Another possibility is that the cross-term effects due to the gradients were not taken into account in the previous work, which might bias the ADC measurements. The increase in ADC of tissue water observed in the older adults in our study is in agreement with literature values obtained previously using DWI (Klimas et al., 2013; Watanabe et al., 2013). It is known that during aging there is a reduction in total dendritic measure (e.g., length, surface area, densities, spine numbers, and branches) (Morrison and Hof, 2003). In addition, it was recently reported using diffusion simulation with data from mouse and macaque brains that a reduction in total dendritic measure would result in decreased ADC values of metabolites (Palombo et al., 2016, 2017), that is, more restricted diffusion. In contrast, ADC values increase (Palombo et al., 2018a) with a loss in dendritic spines only (Dickstein et al., 2013) where the spine space accounts for a small fraction of the total cellular volumes explored by the diffusing metabolites. Interestingly, there is a major reduction in spine densities during aging of the brain (Benavides-Piccione et al., 2012). Based on these findings, we hypothesize that the increase in ADC could in part be attributed to the large spine density decrease with age compared to the other dendritic measures (Palombo et al., 2016, 2017, 2020).

Another possible factor which might explain the increase in ADC findings could be related to the loss of mitochondria (López-Otín et al., 2013) and demyelination (Bennett et al., 2010) with aging. Recently, it has been shown that a small fraction (~5%–10%) of the NAA pool is confined in a highly restricted compartment (Palombo et al., 2017), for example, mitochondrial or myelin pool. During the normal aging process, the relative volume fraction of these restricting structures might decrease, for example, cellular aging leads to loss of mitochondria while demyelination leads to the thinning of the myelin sheath, such that both processes release more NAA, which diffuses freely in the intra-cellular space. Hence, the reduction in volume fraction will lead to an increase in the ADC of NAA consistent with the simulation findings observed in animal brain (Palombo et al., 2017). The higher ADC of mIns with age could be associated with higher relative number of glial cells (Cotrina and Nedergaard, 2002).

The observed age-related differences in ADC values are not readily attributable to differences in the VOI composition between young and older adults. The measured ADC values are averaged values of metabolites contained in GM and WM since CSF does not contain the investigated metabolites. In all VOIs, the percentage of GM was lower and the percentage of WM was higher in older adults than in young adults. In PCC, for instance, GM is 5% lower and WM 5%

Table 2
T_2 values (mean ± SD) of metabolites, tissue water, and water in CSF measured in the 2 age groups in 3 brain regions

Compound	T_2 (ms)								
	PCC			OCC			PFC		
	Young	Older	*p*-value	Young	Older	*p*-value	Young	Older	*p*-value
NAA singlet	322 ± 16	286 ± 14	**9.8×10^{-16}**	304 ± 13	279 ± 17	**5.4×10^{-8}**	355 ± 17	316 ± 25	**1.3×10^{-6}**
tCr-CH_3	183 ± 7	174 ± 7	**7.3×10^{-7}**	178 ± 6	171 ± 7	**0.0004**	194 ± 7	198 ± 11	0.1876
tCr-CH_2	148 ± 7	132 ± 7	**6.1×10^{-14}**	140 ± 6	129 ± 6	**1.7×10^{-10}**	158 ± 9	144 ± 11	**0.0004**
tCho	360 ± 40	332 ± 20	**0.0011**	323 ± 25	314 ± 30	0.3156	442 ± 47	423 ± 33	0.2605
Glu	177 ± 10	171 ± 8	0.0266	177 ± 10	168 ± 13	0.0040	194 ± 11	190 ± 24	0.5993
mIns	206 ± 14	195 ± 10	**0.0007**	184 ± 12	174 ± 11	**0.0018**	235 ± 19	227 ± 17	0.0900
Tissue water	62 ± 3	53 ± 6	**1.4×10^{-8}**	56 ± 3	50 ± 6	**2.7×10^{-5}**	65 ± 2	56 ± 4	**2.3×10^{-13}**
CSF water	250 ± 32	308 ± 102	**0.0082**	225 ± 28	271 ± 34	**5.0×10^{-7}**	280 ± 31	325 ± 43	**0.0004**

Bold values denote statistical significance, i.e. $p < 0.0027$ for metabolites and $p < 0.0083$ for water.
Key: CSF, cerebrospinal fluid; Glu, glutamate; mIns, *myo*-inositol; NAA, *N*-acetyl-aspartate; OCC, occipital cortex; PCC, posterior cingulate cortex; PFC, prefrontal cortex; SD, standard deviation; tCho, total choline; tCr, total creatine.

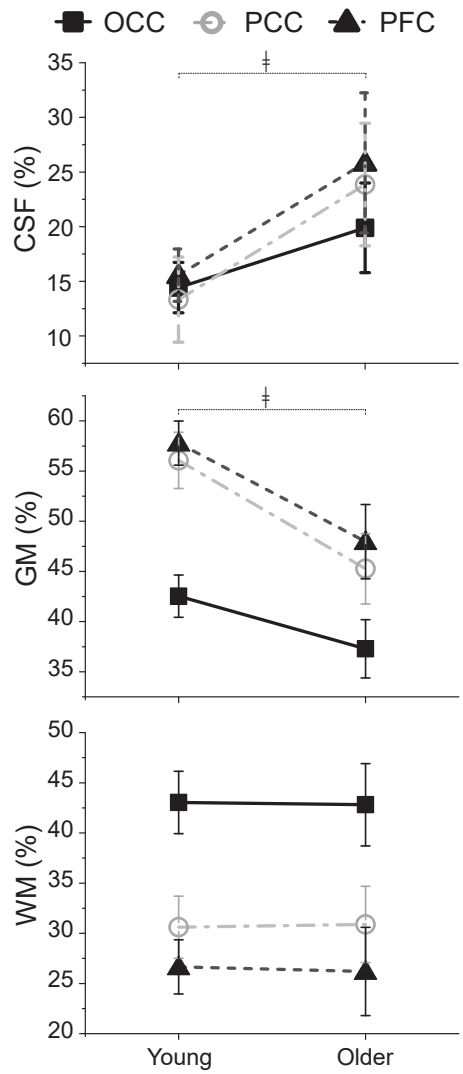

Fig. 3. Means and standard deviations of WM, GM, and CSF content measured in 3 VOIs from T_1-weighted images acquired during the T_2 measurements. * represents statistically significant differences ($p < 0.001$) between young and older adults. Abbreviations: CSF, cerebrospinal fluid; GM, gray matter; VOI, volumes-of-interest; WM, white matter.

higher in older adults relative to young adults. If known ADC values of neurochemicals in GM and WM (Kan et al., 2012; Najac et al., 2016) were used, the differences in ADC due only to difference in VOI composition would be relatively small. For instance, ADC of NAA in PCC would only be 2% higher in older group compared to young group. However, the measured ADC of NAA was 8% higher in the older group (Table 1). As such, difference in tissue composition could only account for a small contribution to the differences in ADC values. Whether age-related ADC differences arise more from GM or WM is beyond the scope of the current study.

T_2 values of metabolites and tissue water were faster and region-specific in the older brains. These findings are consistent with 2 previous studies (Kirov et al., 2008; Marjańska et al., 2013) which reported shorter apparent T_2 relaxation times for NAA, tCr, and tCho with comparable age span to the young and older cohorts used in the present study. Similarly, shorter apparent T_2 value for mIns was observed in our older cohort. It was possible to measure this J-coupled metabolite due to the optimized T_E, high SNR of the spectra, and by taking into account the J-modulation at each T_E during the spectral fitting (Deelchand et al., 2018a). Since mIns is exclusively located in the astrocytes, the age-related difference in T_2 of mIns can be used to monitor metabolic change due to astrogliosis in the aging brain (Cotrina and Nedergaard, 2002).

The shorter T_2 values in older brains might be caused by several factors. This could be due to a change in iron content in the brain, since a strong correlation between iron deposition in the human brain and age exists (House et al., 2007; Mitsumori et al., 2009). Another factor affecting T_2 relaxation could be a reduction in water content in the older adult brain mostly due to atrophy which in turn results in neuronal shrinkage (Chang et al., 1996; Dickstein et al., 2007). Myelin degeneration with age might also account for the loss in T_2 values in late life. The identification of the exact cause of the shorter T_2 in the older brain is beyond the scope of this paper. In our study, the apparent T_2 measured could be affected by the differences in the tissue composition between 2 groups since T_2 of metabolites differ between GM and WM (Mlynarik et al., 2001).

PCC was found to be the most sensitive region for detecting differences in cellular microenvironment with both the ADC and T_2 measurements. This was followed by the OCC and PFC. The fact that PCC shows more advanced differences with age agrees with our recent work where significant neurochemical concentration differences were observed in PCC compared to OCC (Marjańska et al., 2017). PCC is the central hub in the default mode network and is connected to PFC, and decrease in functional connectivity was shown to occur between both regions during aging (Andrews-Hanna et al., 2007; Hafkemeijer et al., 2012). These findings suggest that since different modalities examine different aspects of neurochemicals and water tissue in the brain, it is not straightforward to interpret and link the data together.

The apparent T_2 relaxation time data were found to be more sensitive than the ADC data. This is reflected by the fact that more significant differences in T_2 were observed between metabolites in the studied regions compared to the diffusivity data. One possible explanation is the low number of b-values used in the current study. Using a larger range of b-values might minimize the bias and increase the accuracy in measuring ADC values of metabolites as previously demonstrated in T_2 measurements (Brief et al., 2005). However, this potentially means longer scan time in order to have a reasonable spectral SNR at different b-values when using conventional diffusion sequences with cross-term effects. Another possibility is to use cross-term free sequences (Ligneul et al., 2017) to reduce scan time.

Due to the imposed linewidth criteria of 10 Hz (lower data quality), a small sample size was used in the analysis of the PFC region. This has resulted in not finding significant age-dependent differences in the cellular microenvironment of neurochemicals in PFC between the young and older groups. PFC is known to be a highly vulnerable region to aging based on cellular changes compared to PCC and OCC (Fjell and Walhovd, 2010). In addition, the normal brain ages from the front to the back of the head as evident from previous volumetric MRI (Fjell et al., 2009; Mrak et al., 1997), connectivity maps (Dennis and Thompson, 2014), and glucose uptake measurements (Zuendorf et al., 2003). However, substantial degradation of the spectral linewidth and therefore compromised SNR was observed in most of the acquired PFC data compared to PCC and OCC data. PFC is particularly susceptible to large B_0 variations due to the proximity of the frontal sinuses and nasal cavity. To fully compensate for these B_0 inhomogeneities, higher (2nd and 3rd) order shim corrections are required (Koch et al., 2009). However, commercially available clinical scanners as used in the current study are limited to only having second-order shims and therefore the B_0 inhomogeneities could not be fully compensated in PFC. We hope that high-quality PFC spectra, consistent with current PCC and OCC data quality, will be possible with the availability of higher order shimming hardware in the near future.

5. Conclusion

Intracellular microenvironment differences in neurochemicals in young versus older normal human brains are region-specific as reflected by the ADC and T_2 data. The diffusivity of several metabolites was higher while their apparent T_2 relaxation time constants were shorter in older adults. In conclusion, this study shows that it is feasible to detect differences in the cellular microenvironment of neurochemicals in the normal aging brain and opens up the possibility to investigate the aging process over time.

Disclosure statement

The authors disclose no conflicts of interest.

CRediT authorship contribution statement

Dinesh K. Deelchand: Investigation, Formal analysis, Writing - original draft, Writing - review & editing. **J. Riley McCarten:** Conceptualization, Investigation, Writing - review & editing. **Laura S. Hemmy:** Conceptualization, Investigation, Writing - review & editing. **Edward J. Auerbach:** Resources, Writing - review & editing. **Lynn E. Eberly:** Formal analysis, Writing - original draft, Writing - review & editing. **Małgorzata Marjańska:** Conceptualization, Investigation, Writing - original draft, Writing - review & editing.

Acknowledgements

The authors would like to thank Andrew Oliver and Sarah Bedell for study coordination, Akshay Patke for neuropsychological testing, and Emily Kittelson and Andrea Grant, PhD, for technical support. This work was supported by funding from the National Institutes of Health grants (R21AG045606, P41 EB015894, P30 NS076408).

Appendix A. Supplementary data

Supplementary data to this article can be found online at https://doi.org/10.1016/j.neurobiolaging.2020.07.017.

References

Andrews-Hanna, J.R., Snyder, A.Z., Vincent, J.L., Lustig, C., Head, D., Raichle, M.E., Buckner, R.L., 2007. Disruption of large-scale brain systems in advanced aging. Neuron 56, 924–935.
Benavides-Piccione, R., Fernaud-Espinosa, I., Robles, V., Yuste, R., DeFelipe, J., 2012. Age-based comparison of human dendritic spine structure using complete three-dimensional reconstructions. Cereb. Cortex 23, 1798–1810.
Bennett, I.J., Madden, D.J., Vaidya, C.J., Howard, D.V., Howard Jr., J.H., 2010. Age-related differences in multiple measures of white matter integrity: a diffusion tensor imaging study of healthy aging. Hum. Brain Mapp. 31, 378–390.
Benton, A., Hamsher, K., Sivan, A.B., 1994. Multilingual Aphasia Examination. AJA Associates, Iowa City.
Brief, E.E., Whittall, K.P., Li, D.K., MacKay, A.L., 2005. Proton T_2 relaxation of cerebral metabolites of normal human brain over large TE range. NMR Biomed. 18, 14–18.
Chang, L., Ernst, T., Poland, R.E., Jenden, D.J., 1996. In vivo proton magnetic resonance spectroscopy of the normal aging human brain. Life Sci. 58, 2049–2056.
Christensen, K.J., Moye, J., Armson, R.R., Kern, T.M., 1992. Health screening and random recruitment for cognitive aging research. Psychol. Aging 7, 204–208.
Christiansen, P., Henriksen, O., Stubgaard, M., Gideon, P., Larsson, H.B.W., 1993. In vivo quantification of brain metabolites by 1H-MRS using water as an internal standard. Magn. Reson. Imaging 11, 107–118.
Cotrina, M.L., Nedergaard, M., 2002. Astrocytes in the aging brain. J. Neurosci. Res. 67, 1–10.
de Graaf, R.A., 2007. In Vivo NMR Spectroscopy, 2nd ed. John Wiley & Sons, Ltd, West Sussex, England.
Deelchand, D.K., Auerbach, E.J., Kobayashi, N., Marjańska, M., 2018a. Transverse relaxation time constants of the five major metabolites in human brain measured in vivo using LASER and PRESS at 3 T. Magn. Reson. Med. 79, 1260–1265.
Deelchand, D.K., Auerbach, E.J., Marjańska, M., 2018b. Apparent diffusion coefficients of the five major metabolites measured in the human brain in vivo at 3T. Magn. Reson. Med. 79, 2896–2901.
Delis, D.C., Kramer, J.H., Kaplan, E., Ober, B.A., 2000. California Verbal Learning Test. Psychological Corporation, San Antonio, TX.
Dennis, E.L., Thompson, P.M., 2014. Functional brain connectivity using fMRI in aging and Alzheimer's disease. Neuropsychol. Rev. 24, 49–62.
Dickstein, D.L., Kabaso, D., Rocher, A.B., Luebke, J.I., Wearne, S.L., Hof, P.R., 2007. Changes in the structural complexity of the aged brain. Aging Cell 6, 275–284.
Dickstein, D.L., Weaver, C.M., Luebke, J.I., Hof, P.R., 2013. Dendritic spine changes associated with normal aging. Neuroscience 251, 21–32.
Fjell, A.M., Walhovd, K.B., 2010. Structural brain changes in aging: courses, causes and cognitive consequences. Rev. Neurosci. 21, 187.
Fjell, A.M., Walhovd, K.B., Fennema-Notestine, C., McEvoy, L.K., Hagler, D.J., Holland, D., Brewer, J.B., Dale, A.M., 2009. One-year brain atrophy evident in healthy aging. J. Neurosci. 29, 15223.
Golden, C., 1978. Stroop Experimental Uses. Stoelting, Chicago.
Govind, V., Young, K., Maudsley, A.A., 2015. Corrigendum: Proton NMR chemical shifts and coupling constants for brain metabolites. NMR Biomed. 28, 923–924.
Grieve, S.M., Williams, L.M., Paul, R.H., Clark, C.R., Gordon, E., 2007. Cognitive aging, executive function, and fractional anisotropy: a diffusion tensor MR imaging study. Am. J. Neuroradiology 28, 226.
Grober, E., Sliwinsk, M., Korey, S.R., 1991. Development and validation of a model for estimating premorbid verbal intelligence in the elderly. J. Clin. Exp. Neuropsychol. 13, 933–949.
Hafkemeijer, A., van der Grond, J., Rombouts, S.A.R.B., 2012. Imaging the default mode network in aging and dementia. Biochim. Biophys. Acta Mol. Basis Dis. 1822, 431–441.
Henry, P.G., Marjańska, M., Walls, J.D., Valette, J., Gruetter, R., Ugurbil, K., 2006. Proton-observed carbon-edited NMR spectroscopy in strongly coupled second-order spin systems. Magn. Reson. Med. 55, 250–257.
House, M.J., St. Pierre, T.G., Kowdley, K.V., Montine, T., Connor, J., Beard, J., Berger, J., Siddaiah, N., Shankland, E., Jin, L.-W., 2007. Correlation of proton transverse relaxation rates (R2) with iron concentrations in postmortem brain tissue from Alzheimer's disease patients. Magn. Reson. Med. 57, 172–180.
Jenkinson, M., Beckmann, C.F., Behrens, T.E.J., Woolrich, M.W., Smith, S.M., 2012. FSL. Neuroimage 62, 782–790.
Kan, H.E., Techawiboonwong, A., van Osch, M.J.P., Versluis, M.J., Deelchand, D.K., Henry, P.-G., Marjańska, M., van Buchem, M.A., Webb, A.G., Ronen, I., 2012. Differences in apparent diffusion coefficients of brain metabolites between grey and white matter in the human brain measured at 7 T. Magn. Reson. Med. 67, 1203–1209.
Kaplan, E., Goodglass, H., Weintraub, S., 1983. The Boston Naming Test. Lea and Febiger, Philadelphia.
Kirov, I.I., Fleysher, L., Fleysher, R., Patil, V., Liu, S., Gonen, O., 2008. Age dependence of regional proton metabolites T2 relaxation times in the human brain at 3 T. Magn. Reson. Med. 60, 790–795.
Klimas, A., Drzazga, Z., Kluczewska, E., Hartel, M., 2013. Regional ADC measurements during normal brain aging in the clinical range of b values: a DWI study. Clin. Imaging 37, 637–644.
Koch, K.M., Rothman, D.L., de Graaf, R.A., 2009. Optimization of static magnetic field homogeneity in the human and animal brain in vivo. Prog. Nucl. Magn. Reson. Spectrosc. 54, 69–96.
Kreis, R., Slotboom, J., Hofmann, L., Boesch, C., 2005. Integrated data acquisition and processing to determine metabolite contents, relaxation times, and macromolecule baseline in single examinations of individual subjects. Magn. Reson. Med. 54, 761–768.
Ligneul, C., Palombo, M., Hernández-Garzón, E., Carrillo-de Sauvage, M.-A., Flament, J., Hantraye, P., Brouillet, E., Bonvento, G., Escartin, C., Valette, J., 2019. Diffusion-weighted magnetic resonance spectroscopy enables cell-specific monitoring of astrocyte reactivity in vivo. NeuroImage 191, 457–469.
Ligneul, C., Palombo, M., Valette, J., 2017. Metabolite diffusion up to very high b in the mouse brain in vivo: revisiting the potential correlation between relaxation and diffusion properties. Magn. Reson. Med. 77, 1390–1398.
López-Otín, C., Blasco, M.A., Partridge, L., Serrano, M., Kroemer, G., 2013. The hallmarks of aging. Cell 153, 1194–1217.
Marjańska, M., Deelchand, D.K., Hodges, J.S., McCarten, J.R., Hemmy, L.S., Grant, A., Terpstra, M., 2018. Altered macromolecular pattern and content in the aging human brain. NMR Biomed. 31, e3865.
Marjańska, M., Emir, U.E., Deelchand, D.K., Terpstra, M., 2013. Faster metabolite 1H transverse relaxation in the elder human brain. PLoS One 8, e77572.
Marjańska, M., McCarten, J.R., Hodges, J., Hemmy, L.S., Grant, A., Deelchand, D.K., Terpstra, M., 2017. Region-specific aging of the human brain as evidenced by neurochemical profiles measured noninvasively in the posterior cingulate cortex and the occipital lobe using 1H magnetic resonance spectroscopy at 7 T. Neuroscience 354, 168–177.
McIntyre, D.J.O., Charlton, R.A., Markus, H.S., Howe, F.A., 2007. Long and short echo time proton magnetic resonance spectroscopic imaging of the healthy aging brain. J. Magn. Reson. Imaging 26, 1596–1606.
Meyers, J.E., Meyers, K.R., 1995. Rey Complex Figure Test and Recognition Trial: Professional Manual. Psychological Assessment Resources, Lutz, FL.
Mitsumori, F., Watanabe, H., Takaya, N., 2009. Estimation of brain iron concentration in vivo using a linear relationship between regional iron and apparent transverse relaxation rate of the tissue water at 4.7T. Magn. Reson. Med. 62, 1326–1330.

Mlynarik, V., Gruber, S., Moser, E., 2001. Proton T_1 and T_2 relaxation times of human brain metabolites at 3 Tesla. NMR Biomed. 14, 325–331.
Morrison, J.H., Hof, P.R., 2003. Changes in cortical circuits during aging. Clin. Neurosci. Res. 2, 294–304.
Mrak, R.E., Griffin, W.S.T., Graham, D.I., 1997. Aging-associated changes in human brain. J. Neuropathol. Exp. Neurol. 56, 1269–1275.
Najac, C., Branzoli, F., Ronen, I., Valette, J., 2016. Brain intracellular metabolites are freely diffusing along cell fibers in grey and white matter, as measured by diffusion-weighted MR spectroscopy in the human brain at 7 T. Brain Struct. Funct. 221, 1245–1254.
Nasreddine, Z.S., Phillips, N.A., Bédirian, V., Charbonneau, S., Whitehead, V., Collin, I., Cummings, J.L., Chertkow, H., 2005. The Montreal Cognitive Assessment, MoCA: a brief screening tool for mild cognitive impairment. J. Am. Geriatr. Soc. 53, 695–699.
Öngür, D., Prescot, A.P., Jensen, J.E., Rouse, E.D., Cohen, B.M., Renshaw, P.F., Olson, D.P., 2010. T2 relaxation time abnormalities in bipolar disorder and schizophrenia. Magn. Reson. Med. 63, 1–8.
Palombo, M., Ianus, A., Guerreri, M., Nunes, D., Alexander, D.C., Shemesh, N., Zhang, H., 2020. SANDI: a compartment-based model for non-invasive apparent soma and neurite imaging by diffusion MRI. NeuroImage 215, 116835.
Palombo, M., Ligneul, C., Hernandez-Garzon, E., Valette, J., 2018a. Can we detect the effect of spines and leaflets on the diffusion of brain intracellular metabolites? NeuroImage 182, 283–293.
Palombo, M., Ligneul, C., Najac, C., Le Douce, J., Flament, J., Escartin, C., Hantraye, P., Brouillet, E., Bonvento, G., Valette, J., 2016. New paradigm to assess brain cell morphology by diffusion-weighted MR spectroscopy in vivo. Proc. Natl. Acad. Sci. 113, 6671.
Palombo, M., Ligneul, C., Valette, J., 2017. Modeling diffusion of intracellular metabolites in the mouse brain up to very high diffusion-weighting: diffusion in long fibers (almost) accounts for non-monoexponential attenuation. Magn. Reson. Med. 77, 343–350.
Palombo, M., Shemesh, N., Ronen, I., Valette, J., 2018b. Insights into brain microstructure from in vivo DW-MRS. Neuroimage 182, 97–116.
Peters, R., 2006. Ageing and the brain. Postgrad. Med. J. 82, 84.
Provencher, S.W., 1993. Estimation of metabolite concentrations from localized in vivo proton NMR spectra. Magn. Reson. Med. 30, 672–679.
Reitan, R.M., 1979. Manual for Administration of Neuropsychological Test Batteries for Adults and Children. Neuropsychology Press, Tucson, AZ.
Ronen, I., Valette, J., 2015. Diffusion-Weighted Magnetic Resonance Spectroscopy, eMagRes. John Wiley & Sons, Ltd, New York, United States, pp. 733–750.
Valette, J., Ligneul, C., Marchadour, C., Najac, C., Palombo, M., 2018. Brain metabolite diffusion from ultra-short to ultra-long time scales: what do we learn, where should we go? Front. Neurosci. 12, 2.
van der Kouwe, A.J.W., Benner, T., Fischl, B., Schmitt, F., Salat, D.H., Harder, M., Sorensen, A.G., Dale, A.M., 2005. On-line automatic slice positioning for brain MR imaging. NeuroImage 27, 222–230.
Walhovd, K.B., Westlye, L.T., Amlien, I., Espeseth, T., Reinvang, I., Raz, N., Agartz, I., Salat, D.H., Greve, D.N., Fischl, B., Dale, A.M., Fjell, A.M., 2011. Consistent neuroanatomical age-related volume differences across multiple samples. Neurobiol. Aging 32, 916–932.
Watanabe, M., Sakai, O., Ozonoff, A., Kussman, S., Jara, H., 2013. Age-related apparent diffusion coefficient changes in the normal brain. Radiology 266, 575–582.
Wechsler, D., 1987. Wechsler Memory Scale-Revised. Psychological Corporation/Harcourt Brace Jovanovich, San Antonio, TX.
Wechsler, D., 1997. Wechsler Adult Intelligence Scale, third ed. The Psychological Corporation, San Antonio, TX.
Whittall, K.P., MacKay, A.L., Graeb, D.A., Nugent, R.A., Li, D.K., Paty, D.W., 1997. In vivo measurement of T_2 distributions and water contents in normal human brain. Magn. Reson. Med. 37, 34–43.
Zheng, D.D., Liu, Z.H., Fang, J., Wang, X.Y., Zhang, J., 2012. The effect of age and cerebral ischemia on diffusion-weighted proton MR spectroscopy of the human brain. Am. J. Neuroradiol. 33, 563.
Zuendorf, G., Kerrouche, N., Herholz, K., Baron, J.-C., 2003. Efficient principal component analysis for multivariate 3D voxel-based mapping of brain functional imaging data sets as applied to FDG-PET and normal aging. Hum. Brain Mapp. 18, 13–21.